

Effect of temperature on creep in ASTM A572 high-strength low-alloy steels

Venkatesh K. Kodur · Esam M. Aziz

Received: 20 September 2013 / Accepted: 4 February 2014
© RILEM 2014

Abstract Creep deformations that occur at high temperature can significantly influence the fire response of steel structures. There is limited data on the effect of temperature on creep deformations in structural steel used in construction applications. This paper presents an investigation into temperature induced creep in high-strength low-alloy ASTM A572 steel commonly used in structural members. A set of creep tests is carried out at various stress levels in 400–800 °C range which is commonly encountered temperature range in structures subjected to fires. Results from these creep tests indicate that temperature has significant influence on the level of creep deformations in ASTM A572 steel, especially when the temperature exceeds 500 °C. The extent of creep deformation at a given temperature increases with stress level and the effect can be substantial at 550 °C when the stress level exceeds 50 % of room temperature yield stress. But creep deformations can rapidly rise beyond 800 °C even for low stress levels of about 10–15 % of room temperature yield stress.

Keywords ASTM A572 steel · Mechanical properties · Elevated temperature · High temperature creep · Creep tests

1 Introduction

Steel structures exhibit low fire resistance due to faster loss of strength and stiffness properties of steel and also due to rapid rise in temperatures resulting from high thermal conductivity and low specific heat of steel. The fire resistance of a steel structural member depends mainly on thermal and mechanical properties of steel. Thermal properties that influence fire response of steel structures include thermal conductivity, specific heat, and thermal expansion. Mechanical properties that include strength, elastic modulus, and creep have significant influence on fire response of steel structures. Creep deformations at room temperature are generally low especially in members subjected to low stress levels [1]. However, at high temperatures, creep deformations can become predominant within a short duration of fire exposure and can influence the failure mode and fire resistance of steel structures. The extent of high temperature creep in steel structures primarily depend on properties of steel, exposure temperature, stress level on the member, and time of exposure [2].

Steel used in construction applications are classified into different categories based on chemical composition, tensile properties, and fabrication process as carbon steel,

V. K. Kodur (✉) · E. M. Aziz
Civil and Environmental Engineering, Michigan State
University, East Lansing, MI, USA
e-mail: kodur@egr.msu.edu

E. M. Aziz
e-mail: azizesam@msu.edu

E. M. Aziz
College of Engineering, University of Sulaimani,
Sulaymaniyah, Iraq

high-strength low alloy steels (HSLA), heat-treated carbon steels, and heat-treated constructional alloy steels [3]. High-strength low-alloy steels provide better performance in term of strength, weldability and corrosion/weather resistance. One commonly available HSLA is ASTM 572 Gr. 50 and this steel is widely used in bridge and building applications.

In recent years there have been numerous fires in bridges and some of these fires resulted in the collapse or damage of steel girders [4, 5]. Bridge fire incidents generally occur due to crashing of vehicles in the vicinity of a bridge and burning of gasoline fuel underneath a bridge. These gasoline fires produce severe conditions than that of building fires and are typically characterized by rapid heating rate with peak temperatures reaching to 900–1,100 °C in the first few minutes. Under such conditions creep deformation tends to accelerate at a very rapid rate.

A review of literature indicates that very few experiments have been carried out to study high temperature creep of structural steel. The limited creep tests reported in literature were carried out on ASTM A618, ASTM A992, ASTM A316Ti, A36, AS A149, and SS41 steels and there is no creep data specific to ASTM A572 steel [6–11]. To develop such creep data for fire resistance analysis of structural members [12, 13], this paper presents results from high temperature creep on HSLA ASTM A572 Gr 50 steel at various temperature and stress levels.

2 Creep at high temperature

Steel structures when exposed to elevated temperatures, undergo permanent deformation (plastic) even when applied stress level is below that of yield stress and this time-dependent deformation is referred to as creep. Thus, creep can be defined as an increase in strain in a solid material under constant stress over a period of time. There are two broad mechanisms by which creep takes place in crystalline materials (metals) namely; dislocation creep, and diffusional creep. Dislocation creep occurs due to movement of material dislocations, while diffusional creep is primarily related to transport of material by diffusion of atoms within a grain and could be in two forms namely; grain boundary diffusion and bulk crystal diffusion. The rate of creep strain progression in both these mechanisms depends on the extent of diffusion that occurs in material atoms [14].

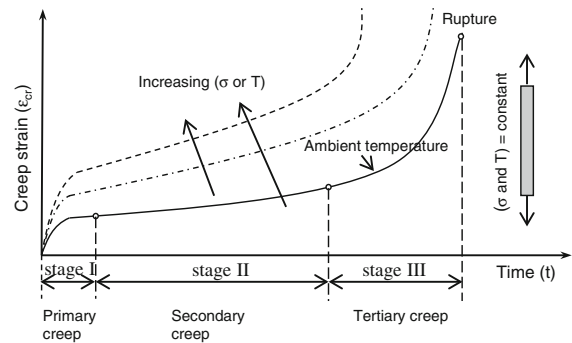


Fig. 1 Classical creep response of steel

Creep deformation occurs due to movement of dislocations in the slip plane. Naturally, metal's (steel) composition contains variety of defects (e.g. solute atoms), that act as obstacles to dislocation motion. At room temperature, creep strain occurs at very slow pace since the amount and distribution of these defects remain almost uniform. At high temperatures, vacancies in the crystalline structure of the material can diffuse into dislocation. This causes the dislocation to move faster to an adjacent slip plane. Therefore, creep deformations in steel accelerate with increase in temperature [2]. The temperatures at which creep deformations accelerate differ in various materials depending on melting temperature and composition of these materials. In general, creep can be significant at temperatures above 40 % of the melting temperature of the material ($0.4 T_m$), where T_m is in Kelvin [7].

Typically, under a constant temperature and stress level, creep behaviour can be grouped into three stages namely; primary (initial) creep, secondary (steady state) creep, and tertiary (accelerating) creep (as shown in Fig. 1) [6]. In Stage I, creep strain starts at a relatively high rate but decreases eventually depending on stress level and temperature. Following that, in Stage II, the strain rate remains almost constant with time. Finally in the last stage (Stage III), creep strain increases at a rapid pace with increase in stress level and this results from necking phenomenon and damage to the material (e.g. formation of microcracks) [14]. However, with increasing temperature and stress levels, rate of creep can become very high and this can lead to significant creep deformations as shown in Fig. 1. Furthermore, with increasing temperature and stress level, it becomes very difficult to distinguish between secondary and tertiary creep stages.

Table 1 Chemical composition of A572 Gr 50 steel as compared to A36 steel

Chemical composition	A36 steel (ASTM limits)	A572 Grade 50 steel (ASTM limits)	A572 Grade 50 steel (Actual)
Carbon (C) %	0.25–0.290	0.23 max	0.06
Manganese (Mn) %	1.03	1.35 max	0.91
Phosphorous (P) %	0.040	0.04 max	0.009
Silicon (Si) %	0.280	0.40 max	0.02
Sulfur (S) %	0.050	0.05 max	0.009
Copper (Cu) %	0.20	–	0.12
Vanadium (V) %	–	0.06 max	0.0818
Cobalt (Co) %	–	0.05 max	–
Iron (Fe) %	The rest	The rest	The rest

3 Experimental studies

A comprehensive test program was designed to undertake creep tests on ASTM A572 steel. The creep tests were carried out at various temperatures in 400–800 °C range and at various stress levels in the range 11–55 % of room temperature yield stress.

3.1 Test specimens

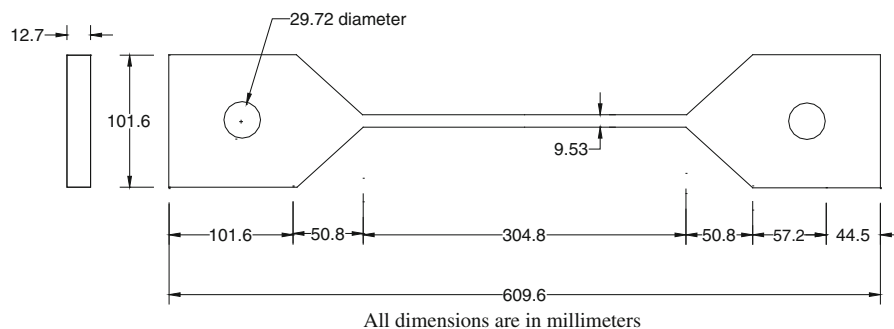
For high-temperature creep tests, rectangular steel coupons were cut from A572 Gr. 50 steel sheets. The chemical composition of A572 steel is different from that of conventional A36 steels. The chemical composition of both types of steel, together with actual composition of A572 steel used in current test program (as specified by the manufacturer) is tabulated in Table 1. The test coupons measured 609.6 mm in total

length and the length of tapered section is 304.8 mm. The cross section of the reduced section is 9.53×12.7 mm. The configuration of a typical test coupon used in creep tests is shown in Fig. 2.

3.2 Test set-up

For undertaking high-temperature creep tests, a custom built integrated load-heating furnace equipment was used. This test set-up comprises of a steel frame for applying tensile loading; a loading lever arm, an electric furnace, and a data acquisition system. The axial tensile load is applied using suspended concrete blocks via the lever arm. The concrete blocks are weighed to determine the magnitude of load. This loading system allows the load to be maintained constant during the entire duration of strength test. The axial deformation of the specimen is measured by a displacement transducer (± 38 mm LVDT), with 0.0254 mm sensitivity, that is placed outside the furnace.

The electric furnace comprises of cylindrical chamber with an inner diameter of 203 mm and a height of 305 mm. Therefore, the heating length of the test specimen is to be 305 mm. The test specimen is mounted between the base steel girder that is fixed to the floor and the top steel girder that moves vertically with the loading arm. The programmable furnace enables generation of target temperatures up to 1,000 °C at a specified rate of temperature rise and keeps the target temperature inside the furnace constant for the duration of strength (creep) test. Three built-in thermocouples are mounted inside the furnace to measure temperatures at upper, middle and lower zones and the average readings of these three thermocouples is taken as the furnace temperature. The furnace and LVDT are connected to a data acquisition system and a

**Fig. 2** Coupon for high-temperature creep tests

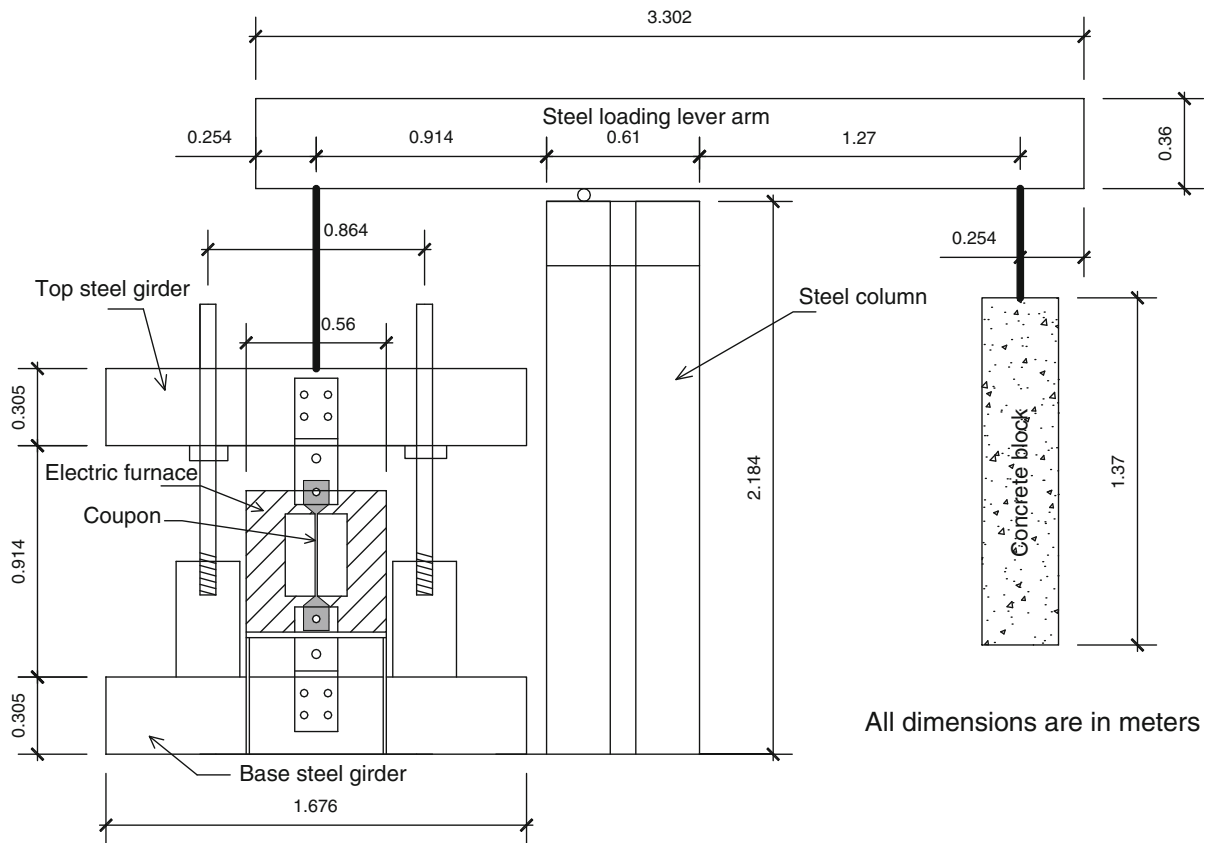


Fig. 3 Schematics of test set-up for high-temperature creep tests

computer wherein temperature and displacements during the test are recorded. A schematic of test set-up for high temperature creep test is shown in Figs. 3 and 4.

3.3 Test procedure

Strength and creep properties of steel at a specific temperature can be evaluated through transient and/or steady-state tests. Although transient-state tests are more realistic in simulating real fire conditions, steady-state tests are more commonly applied due to ease of undertaking these tests. In the current study, steady-state test method was utilized for undertaking high temperature creep tests.

Before undertaking creep tests, tensile strength tests were carried out to evaluate stress–strain response of A572 steel at ambient conditions. These tests were conducted using MTS-810 test machine (depicted in Fig. 5) with 250 kN loading capacity.

Creep tests were conducted at different temperatures and stress levels in the custom built test set-up

described above. For these creep tests, steel coupons were prepared by mounting a thermocouple at mid-length of the tapered cross section as shown in Fig. 6. This thermocouple is to monitor actual temperature progression in the specimen during the creep test. Then, the steel coupon was placed inside the electric furnace and special care was taken to ensure the coupon to be at the centre of the furnace and the loading frame. Following this, a predefined load was gradually applied through a suspended concrete block and this tensile force gets transferred to the coupon through the steel beam (acting as a lever arm). Special care was taken in the design of loading-frame to ensure the loading to be perfectly axial. The total load, that is required to develop a target stress level at the tapered cross section, was applied before heating the specimen.

After few minutes of application of loading, the furnace is turned on to be heated to a target temperature at a heating rate of 10 °C/min. Once the target temperature is attained, the steel coupon was maintained at this temperature for 30 min to attain a steady-

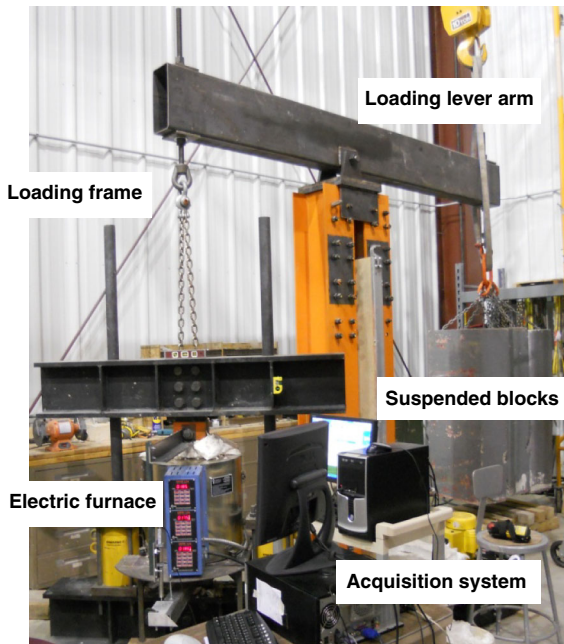


Fig. 4 Custom built creep test equipment for high-temperature creep tests

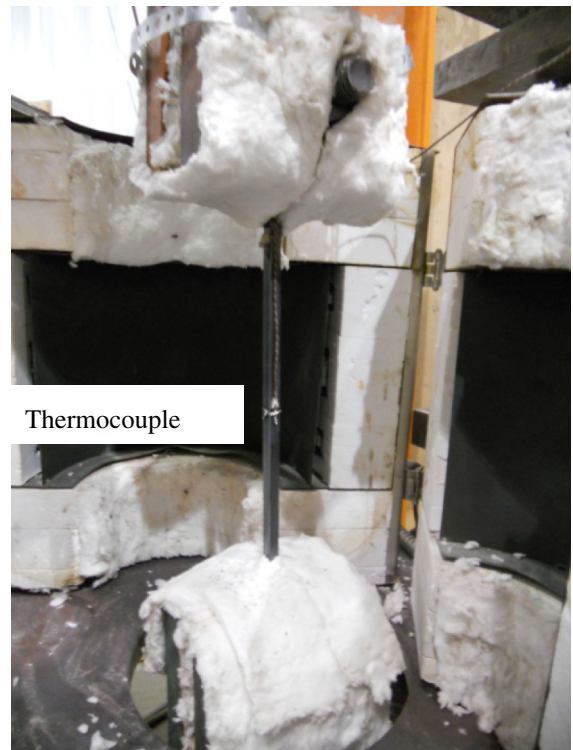


Fig. 6 Coupon placement in the furnace for creep test

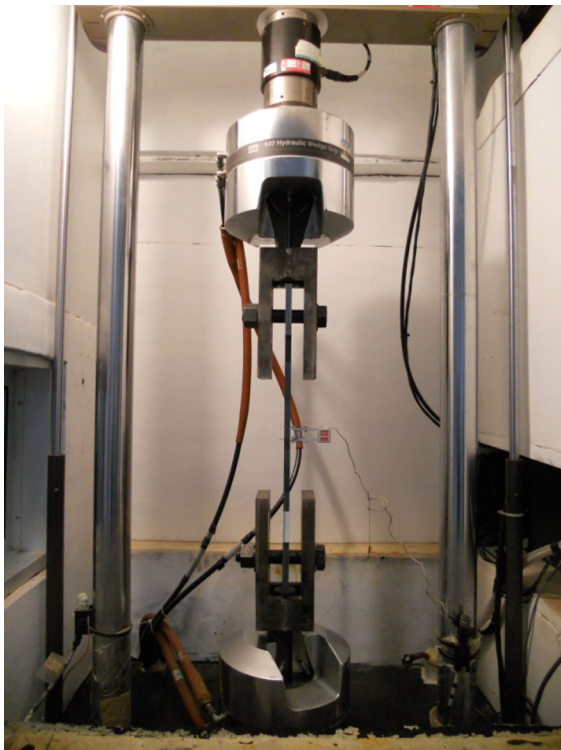


Fig. 5 Test set-up for tensile strength tests

state condition and then the specimen was maintained at the target temperature for the entire test duration. The creep displacement during the test is measured using high sensitive LVDT that is placed outside the furnace. The total length of tapered section of the coupons that is exposed to high temperature during creep tests is 304.8 mm and this is taken to be the gauge length to calculate corresponding creep strain ($\Delta L/L$). Using this procedure, creep tests were conducted at different stress levels and at different temperatures.

4 Results and discussion

Data generated from the above creep tests are utilized to evaluate creep response of A572 steel at various temperatures and stress levels.

4.1 Room temperature stress–strain response

The stress–strain response of A572 steel at room temperature is evaluated using data from uniaxial

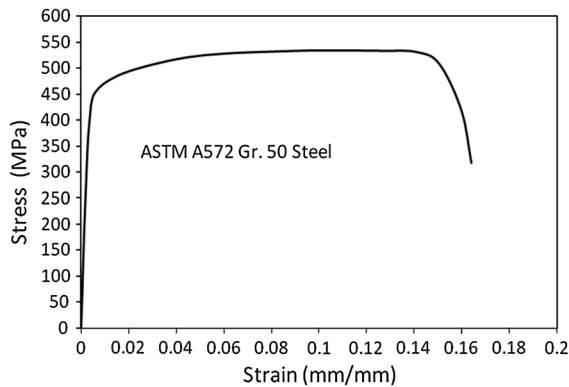


Fig. 7 Stress-strain response of A572 Gr50 steel at room temperature

tensile strength test. The displacements recorded at various load levels, during tension test were used to generate stress–strain response of A572 steel and this is plotted in Fig. 7. It can be seen in the figure that the general trend of stress–strain curve at room temperature is linear-elastic up to yielding of steel at a stress of 453 MPa, followed by nonlinear response. No well defined yield plateau is recorded in the current test on A572 steel unlike that reported in literature [15]. This can be attributed to very low amount of carbon content and also presence of alloy elements such as Vanadium in the chemical composition of steel as shown in Table 1. Once the ultimate stress is reached at a stress of 535 MPa, steel undergoes plastic deformation, through unloading phase up to rupture which occurs at an ultimate strain of 0.165 mm/mm.

4.2 Creep response at elevated temperatures

Data from high temperature creep tests is utilized to derive creep response of A572 steel at various stress levels and temperatures. The stress levels and target temperatures at which these tests were carried out are tabulated in Table 2. The stress level represents ratio of stress due to applied loading to room temperature yield stress.

The measured creep strain at four stress levels is plotted as a function of time in Fig. 8. The general trend of creep response, shown in Fig. 8a–d, can be grouped into two stages, namely secondary (Stage II) and tertiary creep (Stage III). Any primary creep (Stage I) that resulted in these specimens has occurred prior to heating of specimens. Therefore, the initial

Table 2 Selected temperatures and stress levels for creep tests

Stress (MPa)/stress level (%)	Temperatures (°C)			
50/11	600	700	750	800
115/25	500	600	650	700
182/40	500	600	650	–
250/55	400	500	550	–

total strain at the start of heating (time = 0) in creep response curves shown in Fig. 8, represent the sum of mechanical strain from the applied load, thermal strain from heating to target temperature, and strain due to primary creep.

The increase in secondary creep strain with time during Stage II is dependent both on temperature and stress levels. At low stress level of 11 %, there is little secondary creep generated at 500, 600, and 700 °C. However, at higher temperatures of 750, and 800 °C, secondary creep increased at a high rate at this stress level. For moderate stress level of 25 %, the secondary creep starts to dominate at slightly lower temperature of 700 °C. For high stress level of 40 and 55 %, secondary creep increased substantially at temperatures of 600 and 550 °C respectively. The slow rise in creep strain with time in Stage II is due to movement of dislocations that counteract the strain hardening resulting in a balance between strain hardening and thermal softening. Secondary creep is considered to be highly important under fire exposure conditions because it dominates the creep response, occur in a constant rate, and over short period of time.

In Stage III, the tertiary creep increases at a faster rate due to reduced cross section of the specimen resulting from necking phenomenon which results in higher stresses for the same level of applied load. Finally, the material flows and this leads to rupture of specimen under the combined effect of mechanical loading and temperature. At high temperature and stress levels, it becomes difficult to distinguish between Stage II and Stage III of creep because of high creep rate and accelerated flow of material at high temperatures.

A review of results in Fig. 8 indicates that creep deformations are appreciable at temperatures above 500 °C. At a given stress level, the creep deformation increases with temperature. This is due to diffusion of atoms within material grains resulting from temperature rise. When temperatures are in the range of 600–800 °C,

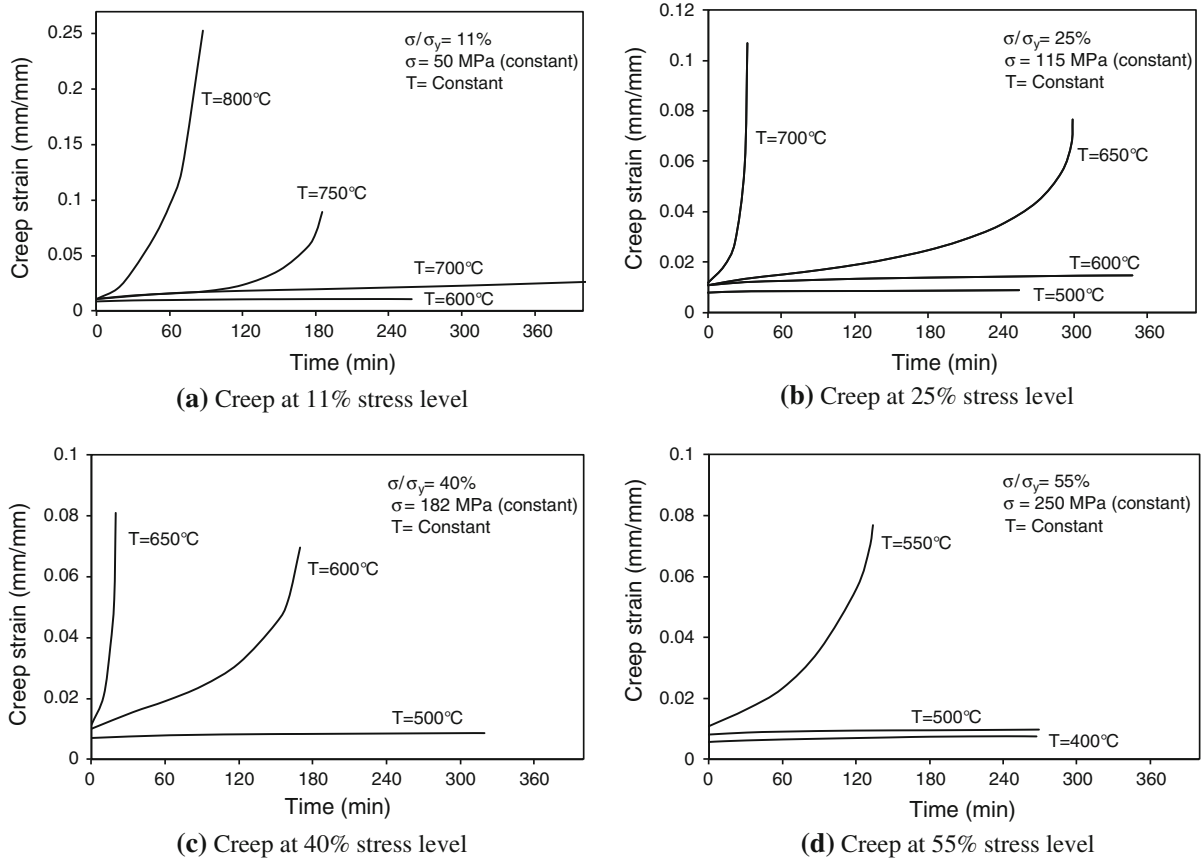


Fig. 8 Creep deformations at various temperatures and stress levels. **a** Creep at 11 % stress level, **b** creep at 25 % stress level, **c** creep at 40 % stress level, **d** creep at 55 % stress level

which represents 30–50 % of steel melting temperature, grain boundary diffusion tends to be the dominant mechanism that results in accelerated creep strain, while bulk diffusion tends to dominate creep deformation in temperature range of 800–1,400 °C (50–99 % of steel melting temperature) [14]. Hence, for the case of 11 % stress level, when steel temperatures rise from 600 to 750 °C, creep strains increase significantly and this leads to rupture of the specimen. Figure 8a–d clearly show that for any stress level, there is a critical temperature at which creep deformations tends to accelerate at a rapid pace and produces failure. This critical temperature typically corresponds to initiation of tertiary creep. Higher the stress level, lower will be the critical temperature.

Different failure modes that resulted in test specimens at various temperature and stress levels are shown in Fig. 9. At higher temperature and under low stress levels, the failure of test specimens was through

a well-defined necking phenomenon, indicating ductile response. For example, failure at 800 °C and stress level of 11 % is in ductile mode since the specimen experienced significant elongation, mainly due to very high creep deformations, before failure. However, at lower temperatures and higher stress levels, the failure was through brittle fracture and this can be seen from flat surface at the mid-length of specimens (see Fig. 9). For example, at 550 °C and stress level of 55 %, the failure is through brittle fracture and mainly due to relatively lower creep deformations.

4.3 Creep response at various stress levels

The effect of stress level on creep response of A572 steel is illustrated in Fig. 10. The creep strain is plotted at temperature of 650 °C for stress levels of 25 and 40 %. It can be seen, for moderate stress level of 25 %, secondary creep increased with time at a constant rate

Fig. 9 Creep failure modes at various temperatures and stress levels. **a** Stress level = 11 %, **b** stress level = 25 %, **c** stress level = 40 %, **d** stress level = 55 %

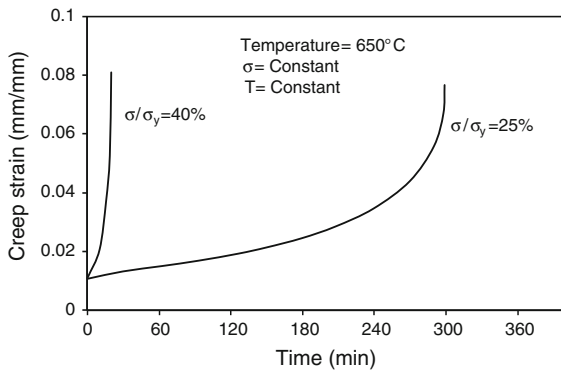
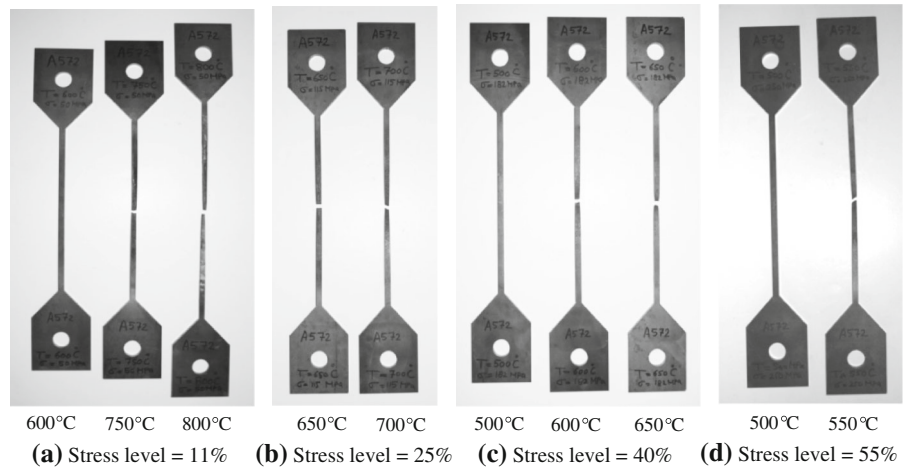


Fig. 10 Creep strain at 650 °C at various stress levels

up to 240 min then the creep strain increased rapidly in the tertiary creep stage up to rupture. However, at 40 % stress level, it becomes difficult to distinguish between secondary and tertiary creep resulting from high creep rate generated due to higher stress level. The trends in the figure indicate that creep deformation increases substantially with increasing stress level. Also, data plotted in Fig. 8d show that creep deformation can be critical for stress levels above 50 % and will produce failure of specimens. Increased creep strain at stress level of 40 % or more can be attributed to dislocation movement due to diffusion of atoms that occur at higher temperatures and under high stress levels.

Figure 11 shows total creep strain just prior to rupture in steel as a function of temperature at four stress levels. The total creep strain at rupture increases with temperature at a given stress level. Furthermore ductility, which is the ability of steel to deform before

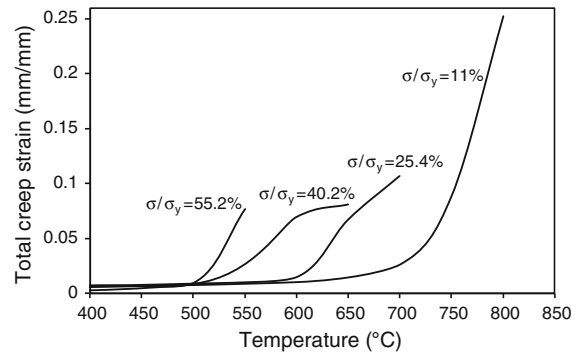


Fig. 11 Total creep strain as a function of temperature

rupture, decreases with increasing stress level. As it can be seen in Fig. 11, the specimens under high stress levels of 40 and 55 % ruptured at lower creep strain than those subjected to lower stress level of 11 and 25 %.

4.4 Design recommendations

Creep deformations can dominate structural response of steel structures under fire conditions, especially when steel temperatures exceed 500 °C. For a specific type of steel, creep strain is mainly dependent on temperature and stress level. Therefore defining a critical temperature limit for creep at different stress levels can be highly useful for evaluating fire response of steel structural members. Critical temperature for creep can be defined as the temperature that corresponds to onset of tertiary creep and this point is an indication of imminent failure of a structural member exposed to fire. Based on test data generated in this

Table 3 Critical temperatures for A572 steel at different stress levels

Stress level (%)	Critical temperature (°C)
11	750
25	650
40	600
55	550

study, the critical temperature for four stress levels are derived as the temperature corresponding to onset of tertiary creep and these values are tabulated in Table 3. Under fire conditions, structural members are typically assumed to be subjected to a loading of about 50 % of room temperature capacity which corresponds to a stress level of 50 % [16]. Hence, stress level beyond 50 % is not of too much interest from the point of fire design of structures.

5 Conclusions

Results of creep tests on high-strength low-alloy ASTM A572 Gr. 50 steel subjected to elevated temperatures are presented in this paper. Based on the results generated from creep tests, the following conclusion can be drawn:

1. Creep deformations in A572 steel is not significant till 500 °C and becomes predominant at temperatures above 500 °C.
2. Creep deformations increase with increasing stress level and become quite predominant when stress levels exceed 50 % of yield stress of steel at room temperature.
3. Increase of temperature by 50 °C, beyond critical temperature of steel, influences creep rate significantly and can alter the failure mode in steel structural members exposed to fire.
4. Creep response tends to be ductile at stress levels below 11 % and temperatures above 700 °C. However, response transforms to brittle mode at stress levels above 50 %.

Acknowledgments This material is based upon work supported by the National Science Foundation under Grant No. CMMI-1068621 and the authors wish to acknowledge NSF's support. Any

opinions, findings, conclusions, or recommendations expressed in this paper are those of the authors and do not necessarily reflect the views of the NSF. The support from University of Sulaimani in the form scholarship to second authors is also acknowledged.

References

1. Cheng L, Ping L, Zhenbo Z, Derek N (2001) Room temperature creep of high strength steel. *J Mater Des* 22:325–328
2. Kodur V, Dwaikat M (2010) Effect of high temperature creep on the fire response of restrained steel beams. *J Mater Struct* 43:1327–1341
3. Brockenbrough RL, Merritt FS (2005) Structural steel designer handbook. McGraw Hill, New York
4. National Steel Bridge Alliance (2010) Steel bridge news. Chicago, USA
5. Astaneh-Asl A, Noble CR, Son J, Wemhoff AP, Thomas MP, McMichael LD (2009) Fire protection of steel bridges and the case of the MacArthur Maze fire collapse. In: Proceedings of the ASCE TCLEE Conference, pp 1–12
6. Brnic J, Turkalj G, Canadija M, Lanc D (2009) Creep behaviour of high-strength low-alloy steel at elevated temperatures. *J Mater Sci Eng* 499:23–27
7. Morovat MA, Lee J, Engelhardt MD, Taleff EM, Helwig TA, Segrest VA (2012) Creep properties of ASTM A992 steel at elevated temperatures. *J Adv Mater Res* 446–449:786–792
8. Brnic J, Turkalj G, Canadija M, Lanc D (2011) AISI 316Ti (1.4571) steel-mechanical, creep and fracture properties versus temperature. *J Constr Steel Res* 67:1948–1952
9. Harmathy TZ (1967) A comprehensive creep model. *J Basis Eng Trans ASME* 89:396–502
10. Knight D, Skinner DH, Lay MG (1971) Prediction of isothermal creep. BHP Melbourne Research Laboratories, Report MRL 18/2, The Broken Hill Proprietary Company Limited Australia, pp 1–14
11. Fujimoto M, Furumura F, Ave T, Shinohara Y (1980) Primary creep of structural steel (SS41) at high temperatures. *Trans Archit Inst Jpn* 296:145–157
12. Kodur VK, Aziz EM, Dwaikat MMS (2013) Evaluating fire resistance of steel girders in bridges. *ASCE Bridge Eng J* 18:633–643
13. Aziz EM, Kodur VK (2012) An approach for evaluating the residual strength of fire exposed bridge girders. *J Constr Steel Res* 88:34–42
14. Ashby MF, Jones DR (2005) Engineering materials I, an introduction to properties, applications and design, 3rd edn. Elsevier Butterworth-Heinemann, Burlington, MA
15. ASM International (2002) Atlas of stress–strain curves, vol 2. ASM, Material Park, OH
16. Franssen J, Kodur V, Zaharia R (2009) Designing steel structures for fire safety. Taylor & Francis Group, London, UK